Spatial Structure and Scale Feature of the Atmospheric Pollution Source Impact of City Agglomeration

Xiangde Xu, Zhaoyang Meng, Guoan Ding, Xiuji Zhou, & Xiaohui Shi

Chinese Academy of Meteorological Sciences, Beijing 100081, China

Abstract The spatial structure and multi-scale feature of the atmospheric pollution influence domain of Beijing and its peripheral area (a rapidly developed city agglomeration) is dissected and analyzed in this paper on the basis of the atmospheric pollution dynamic-chemical process observation data of the urban building ensemble boundary layer of the Beijing City Air Pollution Observation Experiment (BECAPEX) in winter (February) and summer (August) 2003, and relevant meteorological elements and satellite retrieval aerosol optical depth (AOD) etc comprehensive data with the dynamic-statistical integrated analysis of "point-surface" spatial structure. Results show that there existed significant difference in the contribution of winter/summer different pollution emission sources to the component character of atmospheric pollution, and the principal component analysis (PCA) results of statistical model also indicate that SO_2 and NO_X dominated in the component structure of winter aerosol particle; instead, CO and NO_X dominated in summer. Surface layer atmospheric dynamic and thermal structures and various pollutant species at the upper boundary of building ensembles at urban different observational sites of Beijing in winter and summer showed an "in-phase" variation and its spatial scale feature of "influence domain". The power spectrum analysis (PSA) shows that the period spectrum of winter/summer particle concentration accorded with those of atmospheric wind field: the longer period was dominative in winter, but the shorter period in summer, revealing the impact of the seasonal scale feature of winter/summer atmospheric general circulation on the period of atmospheric pollution variations. It is found that from analyzing urban area thermal heterogeneity that the multi-scale effect of Beijing region urban heat island (UHI) was associated with the heterogeneous expansion of tall buildings area. In urban atmospheric dynamical and thermal characteristic spatial structures, the turbulent scale feature of the urban boundary layer (UBL) of architectural complexes had important impact on the multi-scale feature of urban atmospheric pollution. The comprehensive analyses of the variational analysis field of Moderate Resolution Imaging Spectroradiometer (MODIS) AOD-surface PM_{10} under the condition of clear sky and the correlation resultant wind vector field for pollution source-tracing suggest that the emission sources for winter Beijing atmospheric pollution aerosols particle might be remotely traced to the south peripheral greater-scale spatial range of Hebei, Shandong, and Tianjin etc, and the spatial distribution of the high value area of AOD was associated with that of the high value area of resident family number (heating surface source). The backward trajectory feature of winter/summer air particles exhibits analogous multi-scale feature, and depicts the difference in the scale feature of the pollution sources spatial distribution in different season. The peripheral source trajectory paths of urban atmospheric pollution (UAP) mainly come from the fixed industrial surface source or heating surface source in the outskirt of Beijing, and the diffusion and transport distance of peripheral sources in winter is larger than one in summer. The above conclusions depict the multi-scale spatial influence domain and seasonal features caused by UAP source influence and atmospheric dynamical structure. The high value area of the winter Total Ozone Mapping Spectrometer (TOMS) AOD lay in the Beijing region and its south peripheral area, an S-N zonal pattern, which reflects the dynamical effect of peripheral topographic pattern on the diffusion of regional scale atmospheric pollution sources. Study suggests that the extent of winter atmospheric pollution within the "valley"

megarelief in Beijing and periphery was close related with the pollution emission sources of the south peripheral area; and the significant “anti-phase” variation feature of winter AOD and sunshine duration in Beijing and its peripheral areas, and the regional scale correlation of low cloud cover, fog days, and aerosols reflects the local climatic effect of aerosol influence in this region. Besides, analysis of the impacts of atmospheric dry/wet deposition distributions within a valley-scale on the regional water body of Miyun Reservoir also reveals the possible influence of the multi-scale spatial structure of summer water, soil and atmospheric pollution sources on the water quality of Miyun Reservoir.

Keywords: atmospheric pollution source; contribution rate; boundary layer structure; multi-scale; backward trajectory; correlation vector; climatic effect; interaction of water, soil, and atmosphere

In recent years, city population increases sharply (the city population at the beginning of the 21 century is estimated to reach about the 50 % of the total population of the globe), urbanization has become an important background for the local environmental pollution resulted from regional economical development. Facing the severe situation of city environment deterioration, especially the situation of the gradually exacerbation of atmospheric pollution, World Meteorological Organization (WMO) developed the Global Atmosphere Watch (GAW) Urban Research Meteorology and Environment (GURME) programme, and actively studied adaptive measures [1]. Due to the limitation of the detecting means of UBL atmospheric pollutant distribution and the complexity of urban building distribution, it is very difficult to observe the 3-D structure of atmospheric pollutant distribution. Therefore, the visibility data of surface meteorological observations were used to analyze the distribution of aerosols in overseas studies on urban environment [2-4], and in conjunction with boundary layer feature to investigate the dilution/diffusion laws of atmospheric pollutants and the relation of UAP and UHI [5-7].

The “canopy” effect of urban building ensemble plus the specific thermal structure of UHI might result in the particularity and locality of urban local multi-scale circulation and turbulent structure, as well as the multi-scale feature of urban atmospheric environmental structure and the complicated dynamical/thermal structures of UBL, and induce strong convection bubble, and dynamic/thermal turbulent processes [8-10]. Various emitted gases accumulated in the UBL over big city where air is heavy polluted, cover the whole city, and even in conjunction with peripheral areas form a large–scale pollutant cover layer over the city agglomeration. The heterogeneity of the 3-D spatial structure of UBL and its complex turbulent feature result in the mutually feedback effect of the low-level atmospheric pollution processes within UBL. The above UBL structure not only can impact the spatial/temporal evolution of urban local atmospheric pollution, but also form the influence domain of regional atmospheric pollution through the complicated dynamical/thermal structures between city agglomerations. Relevant studies held that the atmospheric pollution of regional and local scales might be spread over city’s peripheral areas, and remotely transported to the downstream area. Under the conditions of particular wind, temperature, and humidity, pollutants are generally transported to the downstream areas in the way of urban plume, which might stretch downstream for several hundred kilometers [11-12].

The Urban atmospheric environment shows the distinctive multi-scale feature. First, the UAP source results in the micro- and regional-scale pollutants transport, and under particular meteorological condition, this pollution might lead to severe harm [13]. In particular, under the interaction of the multi-scale circulation systems of urban atmosphere, the mixing and diffusion of UAP from point, line, and surface sources, through the chemical constituent conversion and photochemical processes of different spatial/temporal scales, form the spatial/temporal multi-scale distributive feature. The large scale transport of pollutants is similar to sand-storm phenomenon, showing a remote transport feature of pollution

crossing-border line, crossing-province, and crossing-region [14-15]. Zhou et al [16] analyzed the critical dynamical issues for the dust-lifting, dust-blowing, dust-transporting, and dust-falling (deposition) processes of the spring sandstorms affecting the Beijing region in 2000, and presented the comprehensive physical model for the dust-lifting, dust-blowing, remote-transporting of the sandstorm activities. Those studies revealed the mutual influence feature of atmospheric pollution processes of different scales from several dozen kilometers to several hundred kilometers. Several cities in the economically developed region may construct a "city agglomeration", and the pollution diffusion and mixing of urban and suburban emission sources or the effect of plumes between megalopolises form the regional large-scale pollution diffusion/mixing phenomenon [17]. According to the actual observation data in U.S.A., the size spectra of atmospheric aerosols in different cities also showed different features: first, the particle number concentration of the photochemical smog aerosols was the highest in Los Angeles, and the lowest in New York- a typical business city where external source influence accounts for the major part of atmospheric pollution; second, the peak values of the size spectra from New York, San Luis to Los Angeles became gradually smaller (particle diameter). The reason is obvious, i.e. the local source in New York is weaker; and external aerosol particles have become rather stable aging particles when arriving at New York in the long distance transport process, the number of external aerosol particles has been reduced, and the size increased due to the collision and aggregation of nuclei mode particles. However, the atmospheric pollution aerosol particles in Los Angeles are mainly generated from photochemical reactions, and their nuclei mode particles result from gaseous and particulate state conversion of automobile exhaust gases. The abundant source for generating nuclei mode particles not only make the number concentration of atmospheric aerosols very high, but also make the peak value of the nuclei mode particle, at which the generating rate is balanced with consuming rate, appear in even smaller size interval [18]. Therefore, atmospheric dynamical/thermal structures also have multi-scale spatial structure features. For example, the large scale synoptic system between cities, sub-synoptic scale UHI, valley wind and sea breeze and other various scale weather systems will significantly impact the physical-chemical processes of UAP, and lead to the multi-scale feature of the influence domains of various urban atmospheric pollution emission sources (point, line, and surface sources)

Based on the above understanding, the "point-surface" combined comprehensive analyses of the atmospheric pollution dynamic-chemical processes observation data of the BECAPEX at building ensemble boundary layer observation sites in winter (February) and summer (August) 2003, the 36 urban automatic weather stations (AWS) data, the NCEP/NCAR reanalysis data, and the satellite retrieval AOD data are performed in the following to depict the spatial structure and its scale feature of UAP source influence, to reveal the contribution of various urban pollution point, line, and surface source emissions to the environmental concentration and their compound impacts, and to preliminarily discuss the regional distribution of atmospheric aerosols and its climatic effect over Beijing and its peripheral areas, and the influence of atmospheric and soil pollution sources on the water quality of reservoir.

1 Brief Introduction to the Field Scientific Experiment of BECAPEX in 2003

The single-point continuous observation of the BECAPEX field scientific experiment was performed at the top of the Main Building (40 m) of Wanshousi Dance College (WDC) in January to April 2003, at the top of the Metering Building (20 m) of China Meteorological Administration (CMA) in April to May 2003, and at the top of the Main Building (50m) of the CMA Training Center in August 2003 to January 2004. Main observation items contain the on-line continuous measurements of PM_{10}, $PM_{2.5}$, SO_2, NO_X, CO, O_3 etc (both WDC and CMA sites are all briefly called "Baishijiao site" hereafter), and the sample time interval for SO_2，NO_X，CO，and O_3 is one minute. The major objective for this observation was to

systematically understand Beijing atmospheric pollution situation, and the possible contribution of peripheral pollution sources to Beijing's pollution.

In order to match with the Atmospheric Chemical Observation in August 2003, the boundary layer observation was also carried out at same time at CMA and south suburb Observatory (briefly called "south suburb site" hereafter), respectively, with the VISALA tethered sonde, and at CMA site the vertical profile observation of O_3 was also performed. Meanwhile, the online continuous measurements of SO_2, NO_2, CO, O_3, and PM_{10} were implemented at the building top (50m) of Institute of Geographical Science and Natural Resource Research, Chinese Academy of Sciences (IGSNRR, CAS) near the Olympic Center, and south suburb site (see Fig.1).

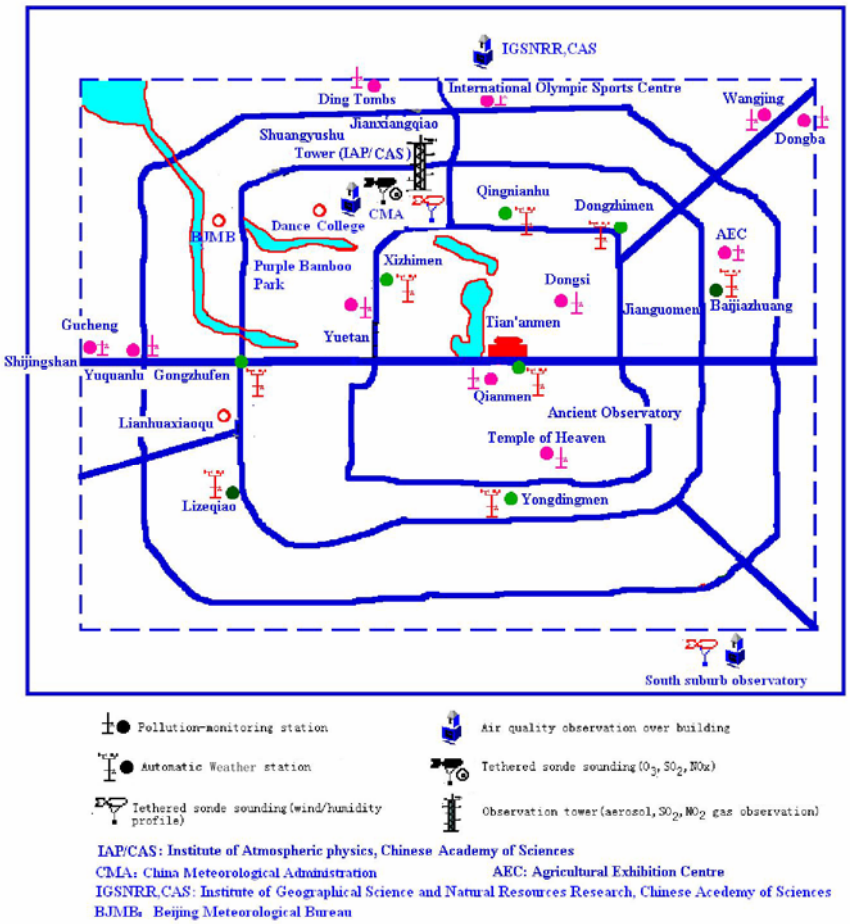

Fig.1 Station site layout of the Beijing Atmospheric Boundary Layer Physical-Chemical Monitoring Experiment of 2003 BECAPEX Summer Experiment

2 Principal component structures of aerosol particle and atmospheric pollution source impact

Relevant study [19] points out that the analyses of the local source emission rates of Beijing urban various pollutant local emission sources and their contribution rates to the environmental concentration suggest that power plants, heating, and industrial surface source were three major emission sources of SO_2, and automobiles, power plants and industries three major emission sources of NO_X.

In the empirical orthogonal function (EOF) decomposition, irregular grid points form a spatial point set of stochastic variable samples, i.e. samples or objects for PCA, and then, view variable matrix $X_{m\times n}$, which consists of the observations of n times at m spatial points, as the linear combination of p spatial eigenvectors and their time weight coefficients [23]:

$$X_{m\times n} = V_{m\times p} T_{p\times n}, \quad (1)$$

where T is the associated time coefficient (ATC), and V the spatial eigenvector. After decomposed using the EOF analysis, the major information of the variable field is extracted and represented by several typical eigenvectors. For j^{th} observation value x_{ij} at i^{th} observation station, EOF expansion is to decompose x_{ij} into the sum of products of spatial functions and temporal functions:

$$x_{ij} = \sum_{k=1}^{m} v_{ik} t_{kj} = v_{i1} t_{1j} + v_{i2} t_{2j} + \cdots + v_{im} t_{mj}, \quad (2)$$

The PCAs of winter/summer PM_{10}, $PM_{2.5}$ particle concentration time series, and various gaseous pollutant concentration sample series at Baishiqiao site in 2003 BECAPEX were performed, yielding eigenvectors depicting the component combinations of various pollutant species and their variance contributions (VC). According to the correlation between winter/ summer PM_{10} and $PM_{2.5}$ concentrations and the ATC of the eigenvector of the component combination of various pollutant species, and the ratios of the VCs of principal components, the first EOF eigenvector coefficient matrix (FEM) of four species gaseous pollutants of PM_{10} and $PM_{2.5}$ principal components can be selected and listed in Table 1.

The FEM of principal components in Table 1 can depict the component ratios of various gaseous pollutant species of winter/summer PM_{10} and $PM_{2.5.}$ The ratios of the component combination of four species gaseous pollutants corresponding to winter PM_{10} and $PM_{2.5}$ are the first eigenvector coefficients on the first and second line of the matrix, respectively. That is to say, first line:0.529, 0.429, 0.530, -0.504; and second line: 0.534，0.419，0.535，-0.503. Those coefficients depict orderly the size of the "weight" coefficient of the principal component combinations of NO_X，CO，SO_2，and $O_{3.}$ The third column (SO_2) coefficients on first and second lines of the principal component eigenvector of winter PM_{10} and $PM_{2.5}$ are the largest, the first column (NO_X) coefficients next, the fourth column (O_3) coefficients third, and the second column (CO) coefficients fourth. Those describe that the impact of SO_2 and NO_X dominated in the principal component of winter PM_{10} and $PM_{2.5}$, and the next was O_3 and CO. Similarly, in the FEM of summer PM_{10} and $PM_{2.5}$, the second column (CO) coefficients are the largest, and the first column (NO_X) coefficients next. Therefore, the impact of CO and NO_X dominated in the principal component of summer PM_{10} and $PM_{2.5}$ particles. The above principal component "weight" coefficients of winter/summer PM_{10} and $PM_{2.5}$ particle pollutant species influences reflect the seasonal features of the correlation structure of gaseous and particulate states in Beijing urban atmospheric pollution source impact processes, and the analysis conclusion also depicts the seasonal difference of urban pollutant emission source impact.

Table 1 Eigenvector coefficient matrix of the component combination of four species gaseous pollutants corresponding to the principal component of winter/summer PM_{10} and $PM_{2.5}$ observed at Baishiqiao site

1st Eigenvector		NO_X	CO	SO_2	O_3
Winter	PM_{10}	0.529	0.429	0.530	-0.504
（Feb）	$PM_{2.5}$	0.534	0.419	0.535	-0.503
Summer	PM_{10}	0.597	0.617	0.418	-0.295
（Aug）	$PM_{2.5}$	0.596	0.610	0.426	-0.303

3 Phase features of the spatial/temporal variations of atmospheric pollution in UBL "canopy"

The analysis [20] of the data at Linan background atmospheric pollution observation station indicated that when wind was small, the photochemical reaction controlled by solar radiation was the

dominant factor affecting the concentrations of O_3 and NO_X; the daily mean O_3 concentration was higher on clear sky or cloudy days, lower on overcast or rainy days, and the impact of temperature on O_3 concentration was smaller; under the conditions of different weather, the diurnal variation of O_3 concentration had a similar single-peak pattern feature, while the diurnal variation of NO_X concentration showed a double-peak pattern. And it was also pointed that the biomass burning was the major local emission source of NO_X in rural areas. Research results[21-23] also revealed the periodic features of the distinctive double-peak pattern diurnal variation etc of the atmospheric pollutant concentrations of NO_X, SO_2, and CO etc in the Beijing region, and presented the conception of seasonal variations of atmospheric pollution.

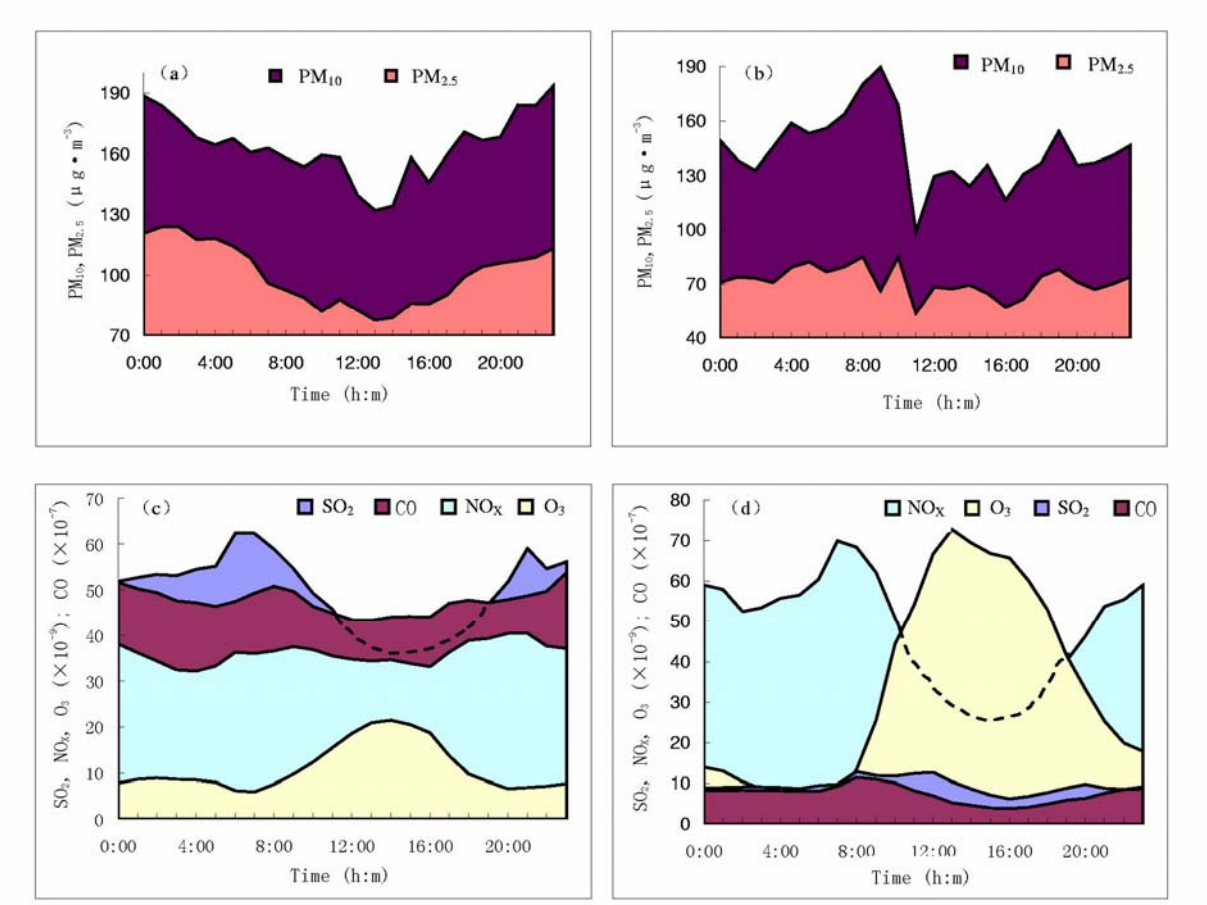

Fig.2 Diurnal variations of winter (February, 2003)/summer (August, 2003) suspended particle matter and four species gaseous pollutants at Baishiqiao site. (a) winter suspended particle matter; (b) summer suspended particle matter; (c) winter gaseous pollutants; (d) summer gaseous pollutants

Mean diurnal variations (Fig.2) of winter (February, 2003)/summer (August, 2003) PM_{10} and $PM_{2.5}$ particle concentrations and four species gaseous pollutant concentrations at Baishiqiao site were calculated in order to further analyze the periodic character of winter/summer diurnal variation time scale of atmospheric pollution. It can be seen from Fig.2 that winter/summer atmospheric pollutants both exhibited diurnal variations: winter PM_{10} and $PM_{2.5}$ particle concentrations at Baishiqiao site exhibited a diurnal variation of single-peak pattern with the peak value at about 00:00 LT (Fig.2(a)), and SO_2, CO, and NO_X concentrations a diurnal variation of double-peak pattern with the two peaks at 21:00 LT and in about 06:00-08:00 LT, respectively (Fig.2(c)). Summer PM_{10} and $PM_{2.5}$ particle concentrations also displayed a diurnal variation of double-peak pattern (24, 12 h periods) with the two peaks at 08:00 and 20:00 LT, respectively, but the principal peak at about 08:00 LT(Fig.2(b)), and NO_X, CO, and SO_2 concentrations still

displayed a diurnal variation of double-peak pattern with the two peaks at about 00:00 and 08:00 LT respectively (Fig.2(d)). Winter/summer O_3 concentrations peaked at about noon, showing a diurnal variation of single-peak pattern. The distinctive difference of the diurnal variations of winter/summer atmospheric pollutants may reflect the impact of winter/summer different pollutant emission sources.

The analysis results of the spatial/temporal variations of the atmospheric pollution data of BECAPEX observed at the top of four tall buildings at different sites across the Beijing urban area from January to March 2001 reveal that the overall impact of urban-scale emission sources in the heating season was significant, and the staggered impact of winter heating period/non-heating periods of urban emission sources also significant; the concentrations of pollutants NO_X, SO_2, and CO at the upper boundary of building ensemble (at the top of buildings) had the "in-phase" temporal evolution feature over a large area of city-regional-scale. O_3 concentrations at different sites had the same variation trend but in a reversed phases with above pollutants. Pollutants in heavy pollution processes in the heating and non-heating seasons also had the synchronous variation trend. Different studies [24,25] draw the same conclusion that the atmospheric pollutants at different sites of Beijing urban area had the "in-phase" variation trend. Fig.3 shows that the atmospheric pollutant species (CO, SO_2, NO_X, O_3) at different sites (IGSNRR, CMA, and south suburb site) within the urban-scale range in the summer experiment stage of BECAPEX also had the significant "in-phase" feature, i.e. the atmospheric pollution shows a synchronous variation feature of urban spatial scale. It can be also observed from Fig.3 that the amplitude of NO_X concentration at south suburb site in part of the period was more remarkable than one at the urban area, thus reflecting the local pollution impact character of different sites. Besides, on the average, SO_2 concentration at Olympic sports center (IGSNRR, CAS) site in the north of Beijing urban area was higher than those at Baishiqiao (the CMA Training Center) site and south suburb site, which may reflect the impact of local emission source impact.

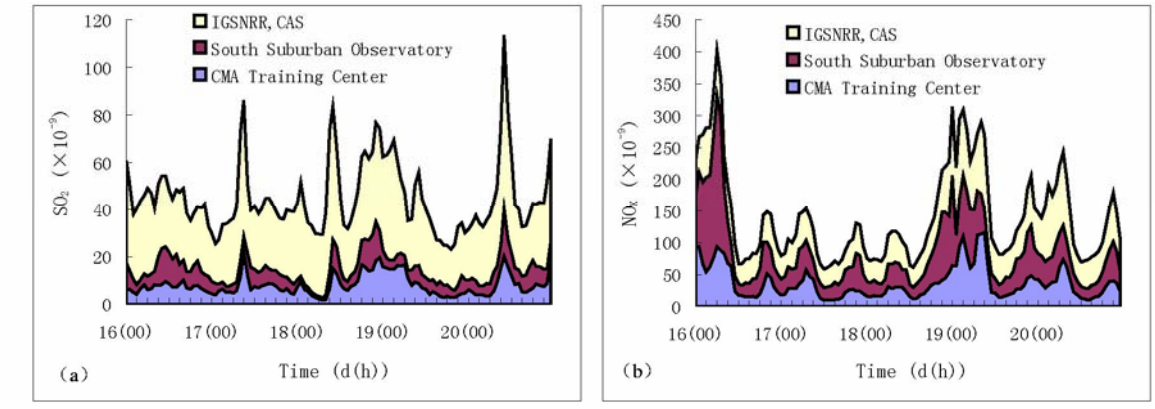

Fig.3 Comparison of hourly mean concentrations of SO_2 (a) and NO_X (b) at different sites from 00:00 LT 16th to 23:00 LT 20th August 2003

It is found from the analysis of hourly concentration variations of SO_2 and NO_X at Shuangyushu, Beijing Meteorological Bureau (BJMB), and Lianhuaxiaoqu sites from 00:00 LT 8th to 22:00 LT 20th January 2001 (Fig.4) that the winter atmospheric pollution variation was similar to one in summer, i.e. it showed an "in-phase" variation feature. Comparing Fig.3 with Fig.4 shows that the amplitudes of winter/summer atmospheric pollution concentrations at different sites were different, and winter amplitude was larger than summer one.

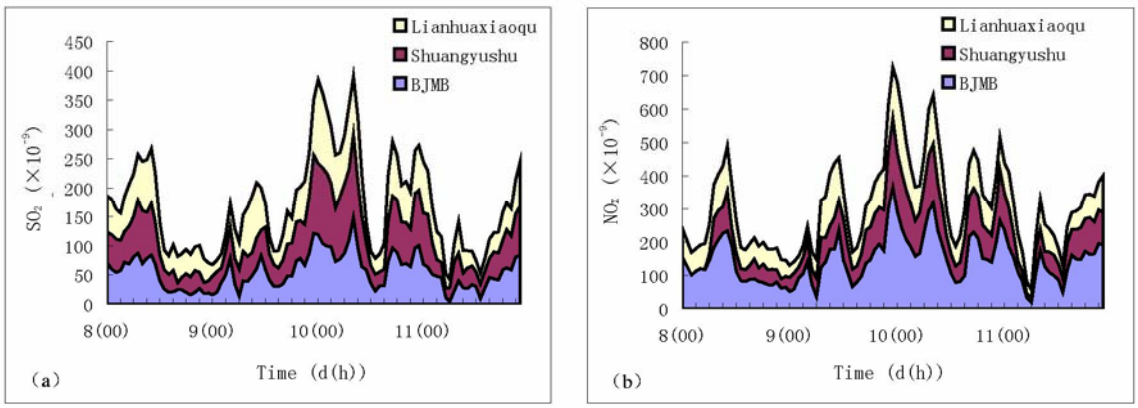

Fig.4 Comparison of hourly mean concentrations of SO_2 (a) and NO_X (b) at different sites from 00:00 LT 8th to 22:00 LT 11th January 2001

The correlation coefficients of winter (January 2001) /summer (August 2003) various pollutant species at the top (50-80 m height) of tall buildings at different sites were calculated using the observation data of BECAPEX, and it can be found from calculating results that winter/summer various pollutant species at the upper boundary of the "canopy" of building ensemble both showed a significant regional correlation of city-scale, especially, the winter correlation at different sites was very significant, and on the whole, the correlation of the in-phase variations of winter various pollutants was higher than that of summer pollutants. Meanwhile it can also be seen that the regional correlation of winter SO_2 concentrations was most distinctive, those of CO or O_3 were next, and that of NO_X was relatively worse; however, the "synchronism" of O_3 and CO concentration variations at different sites was more distinctive than other pollutant species. On the whole, the correlation of city-scale of summer SO_2 was far lower than other three species. The above seasonal characters of various pollutant species can depict that the large-scale diffusion and transport of winter soot type pollutants (SO_2 etc) resulted in the significant spatial structure feature of regional in-phase variations, while the locality of summer emission sources was stronger (Figure omitted)

Atmospheric pollution processes are close related with the dynamical/thermal structures of UBL, and urban heavy pollution processes frequently take place under the typical weather background whose boundary layer has such a dynamic/thermal structures to suppress the diffusion of atmospheric pollutants. Therefore, UBL wind and temperature etc element fields will control and constrain the spatial /temporal variations of UAP. Tiananmen, Olympic sport center, Gongzhufen, Baijiazhuang, and the Temple of Heaven were selected as AWS sites representative of urban area，and variations of hourly mean wind speeds in winter (January, 2001) and summer (August,2003) during BECAPEX at various sites were analyzed (due to missing data, only the wind speeds at Tiananmen, Gongzhufen, Baijiazhuang sites were analyzed in January 2001, Fig.5). Analysis results suggest that wind speed variations at different sites showed a distinctive "in-phase" feature. Besides, temperatures at different sites also showed a similar "in-phase" variation feature (Figure omitted). However, it must be pointed out that there were a lot of small-scale oscillations of short periods in the AWS wind speed records due to the urban surface layer AWS record reflects the complicated dynamical/thermal characters of the underlying surface. If the time-running filter is used, the "in-phase" feature of variations of the dynamical structure of city-scale will be more distinctive. Therefore, it can be found from analyzing and comparing the mean wind speeds of AWS at different sites in urban area with the evolution character of atmospheric pollutant SO_2 and NO_X etc concentrations at the upper boundary (the top of buildings) (Figs.3, 4, and 5) that the both did show the similar " in-phase" evolution feature of city-regional-scale.

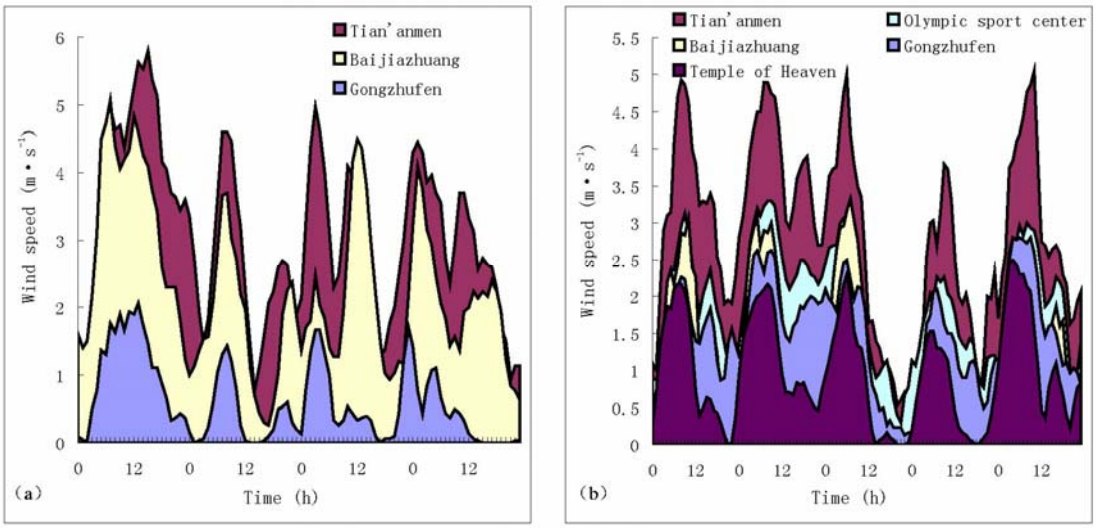

Fig.5 3-h running mean values of winter/summer hourly averaged AWS wind speeds at urban different sites. (a) winter, 00:00 LT 8th to 23:00 LT11th January 2001; (b) summer, 00:00 LT 16th to 23:00 LT 20th August 2003

The above computational results suggest that the "in-phase" feature of atmospheric pollution variation at the upper boundary of urban building ensemble might be correlated with the regional "in-phase" variations of dynamic/thermal factors in the surface layer. The above atmospheric pollution variation laws reveal the regional feature of UBL atmospheric variations and the transport and mixing effects of turbulent-scale, and also suggest that the synchronous variations of city-regional-scale of meteorological elements at urban different sites might be a dynamical background condition for the "in-phase" variation of atmospheric pollution. The above "in-phase" variation laws of the city-regional-scale of atmospheric pollution at different sites could be used to develop new prediction method for air pollution in the "point-surface" combined approach, i.e. to establish the "point-surface" combined statistical model which can depict the "in-phase" correlation feature of atmospheric pollution between single point (representative station) and its peripheral sites. The above analysis conclusion of "point-surface" combination "in-phase" variation may provide the theoretical evidence for atmospheric dynamic-chemical coupling model products and the application of statistical-dynamic technique approach.

4 Spectral characters of urban aerosol concentration variations

The statistical analysis method is employed to reveal the multi-scale periodic characters of atmospheric pollution process, and the PSA of winter (February, 2003)/summer (August, 2003) AWS wind, temperature continuous record, and PM_{10} time series (672, and 360 samples, respectively) were performed. The Fourier transformation of time series auto-correlation function is used to indirectly estimate the power spectrum. At first, the auto-correlation function is computed:

$$r_\tau = \frac{1}{n-\tau}\sum_{t=1}^{n-\tau} X_t X_{t+\tau} \qquad (\tau = 0, 1, 2, \cdots, m), \tag{3}$$

where m is the maximum time lag, the rough estimation of power spectrum D_j ($j = 0, 1, 2, \ldots, m$) is then calculated, and the rough spectral estimation smoothed with the following expressions:

$$\begin{cases} \hat{D}_0 = 0.5D_0 + 0.5D_1 \\ \hat{D}_j = 0.25D_{j-1} + 0.5D_j + 0.25D_{j+1} \qquad (j=1, 2, \cdots, m\text{-}1), \\ \hat{D}_m = 0.5D_{m-1} + 0.5D_m \end{cases} \tag{4}$$

at last, the significant test for smoothed power spectrum is performed, and the significant period of time series determined.

Figs.6 (a) and (b) display the power spectra of winter/summer PM_{10} particle concentrations and the spectrum density curve of red noise test, and it is known from Fig.6 that winter/summer PM_{10} particle concentrations both showed the short period of several hours, and the leading three principal periods of winter PM_{10} particle concentration were all the "long period" of several days, which is consistent with the decaying period of about 10-day of aerosol particulate matter [25], reflecting the remote large-scale transport feature of winter PM_{10} particles and its effect. However, in summer except the individual principal period of about 12-h, most of principal periods were all the short periods of 2-3 h. The above results reflect the differences of winter/summer different emission sources and climatic difference, i.e. distinctive differences in the "soot" type emission source in the heating season in north China and climatic background etc.

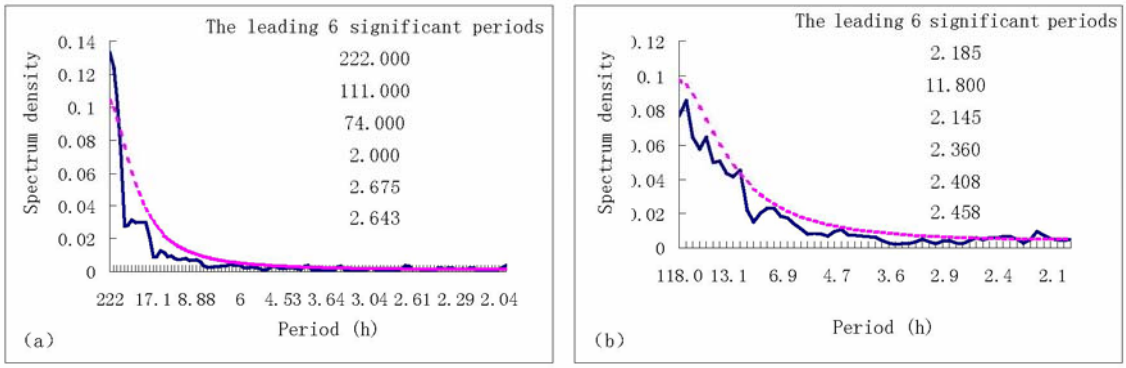

Fig.6 Power spectra of winter (a; February, 2003)/summer (b; August, 2003) PM_{10} particle concentration time series at Baishiqiao site. The dash line denotes the $\alpha=0.05$ red noise standard spectrum.

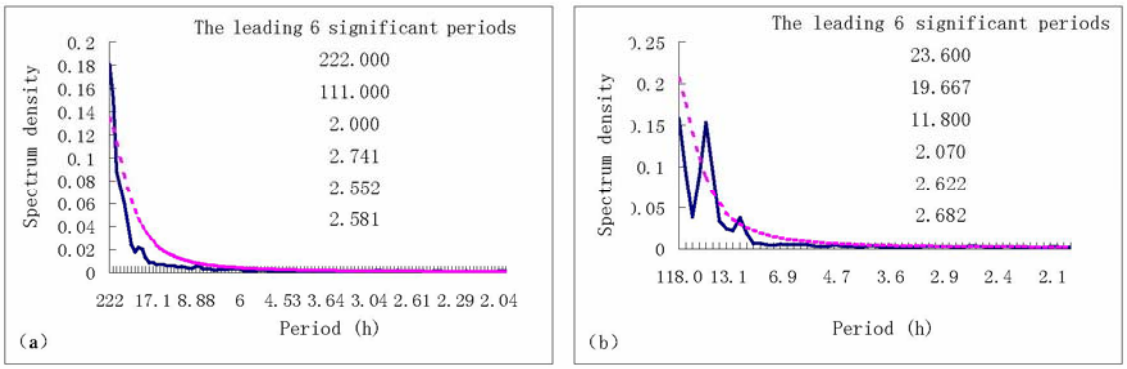

Fig.7 Power spectra of winter (a; February, 2003)/summer (b; August, 2003) meridional wind speed time series at Zizhuyuan site. The dash line denotes the $\alpha=0.05$ red noise standard spectrum.

In order to investigate the scale character of the periods of the correlation between the local wind field of winter/summer atmospheric general circulations and atmospheric aerosol particle matter distributions, the PSA of the meridional component time series of winter/summer winds of Zizhuyuan AWS at Baishiqiao site was performed. It can be observed from Fig.7 that the diurnal variation and 2-3 h short period variation of meridional wind were significant in summer local wind field; however the several-day long period variations were dominant in winter, and others were the short periods of 2-3 h. The winter long period is consistent with the evolution period of winter PM_{10} particle concentration. The above phenomenon reveals the periodic character differences of urban local wind field variations under the winter/summer atmospheric general circulation backgrounds, i.e. the large-scale system periodic character of winter local wind field was more distinctive than one of summer. The impact of the seasonal feature of atmospheric circulation

system evolution on the period of aerosol PM_{10} concentration might lead to the particular long period variation process of winter atmospheric pollution PM_{10} particle concentration differing from summer. The phenomenon also reveals that winter urban aerosol particle matter concentration variation processes had a longer decaying period than summer.

5 Multi-scale spatial structure feature of UHI

In the recent 20 years, Beijing city has rapidly developed, its range greatly expanded, the load increased, and the quantity and height of buildings also increased, and those changes will impact Beijing UBL character. In the recent years, a series analysis studies of observational and historical data and researches on Beijing UBL have been made, and found that the Beijing UHI is strengthening, and the surface roughness and displacement height are growing [27], and some new knowledge [28] of Beijing UBL wind and temperature profiles features has been obtained, but many problems on atmospheric turbulent features and energy budget still remain to be investigated.

It is found from the statistical analysis of the 1962-2000 data that differences of urban-suburban temperatures were significantly correlated with urban manufactured floor space (MFS), and their CC reaches 0.42, passing 0.95 significant test, which suggests that the rapidly development of Beijing urbanization has resulted in the gradually significant overall effect of UHI (Fig.8). The analysis of the building block's distribution of 200m×200m resolution shows that the density and height of urban buildings both exhibited a non-uniform distributive feature, tall building (more than 45 m) mainly concentrated in Shijingshan District, the southwest of Haidian, Xicheng District, the south of Chongwen, the northeast of Chaoyang District etc, while most of architectural complexes in the central zone along the axle wire of ancient city, and the north park and garden area of Haidian District were building ensembles lower than 45 m (Figure omitted).

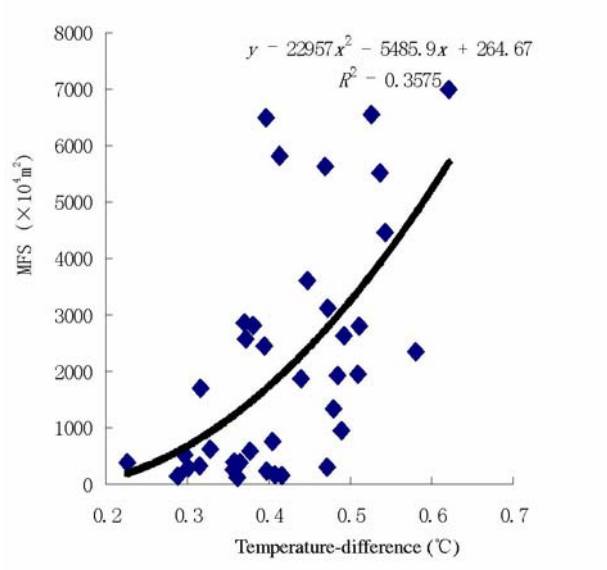

Fig.8 Scattering diagram of urban-suburban temperature differences and MFS in Beijing over 1962-2000

The monthly mean surface air temperature distribution of October 2003, obtained from the composite analysis of the temperature data of conventional and AWS stations, reveals that the Beijing region UHI on the whole broke into the east and west side areas, and a south significant "strong UHI" area (the multi-scale feature of the non-uniform distribution of UHI), and the east of the city center was a "weak UHI" belt, i.e. the narrow belt east of the ancient city axle wire was a relatively lower value area of surface air temperature(Fig.9(a)). It can be found from comprehensively analyzing UHI and building group distributions that there existed some relation between tall building groups and the above multi-scale (or

non-uniform) feature of UHI in Beijing urban area. The relevant study [29] on the city-scale UHI feature of Beijing and its surrounding area and its evolution also found that the interdecadal enhancing area of HU effect in Beijing accorded well with the expansion area of urban building groups. The above UHI multi-scale feature of urban thermal non-uniform distributions (several "high temperature" or "low temperature" centers) depicts the complicated "canopy" non-uniform thermal structure of urban building groups, then under the background condition of multi-scale UHI, did the spatial structure of regional flow field significantly response or not? Was the mesoscale circulation feature in the urban area significantly correlated with the structural non-uniformity?

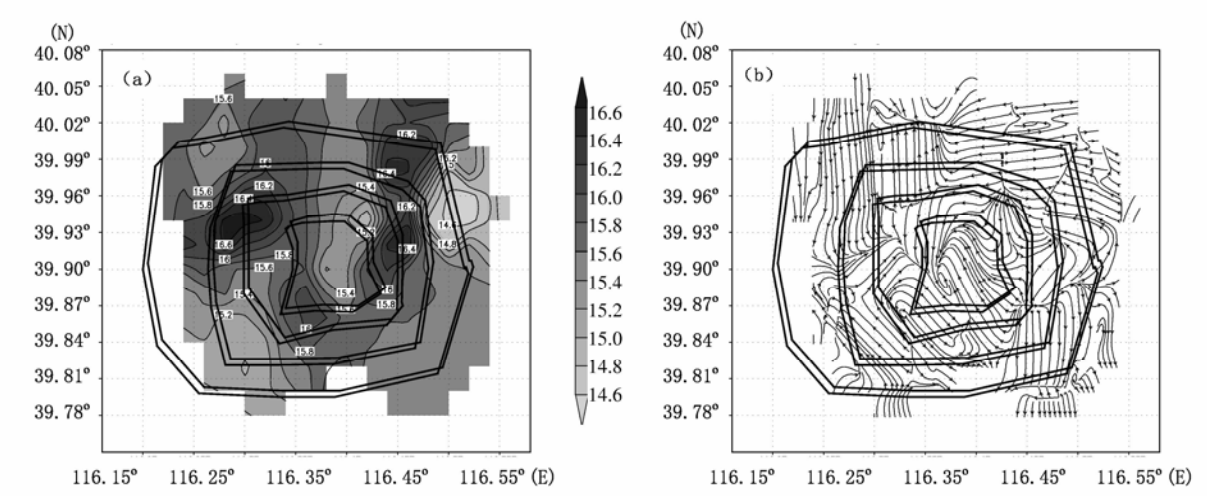

Fig.9 The monthly mean surface air temperature (a; unit: ℃) and filtered wind field streamline (b) distributions of October 2003 obtained from the composite analyses of Beijing city meteorological station and AWS stations data.

The monthly mean filtered wind field (Fig.9(b)) is obtained from the composite of filtered daily wind fields at 32 conventional and AWS stations within Beijing urban area in October 2003, and it can be seen from Fig.9(b) that the convergent flow area of block-scale in Beijing urban and outskirt areas lay in the central-east of Haidian District, Shijingshan District, the northeast of Chaoyang District etc, which accords basically with the distribution of the "strong UHI group"; and the significant divergent flow area in the park and garden green-belts of summer palace etc in the north of Haidian and areas north and east of the axle wire of ancient city, which corresponds to the "weaker UHI" area. The above research result indicates that under the impact of the non-uniform feature of the multi-scale effect heat islands of urban building ensemble, the local convergent area of urban mesoscale low systems and the local UHI vertical circulation might form in the UBL. Such a "UHI forcing circulation" possesses the small-scale system character. If the building groups relatively concentrate in urban areas or city agglomerations, multi-UHI forcing circulations of relatively smaller-scale, and different intensities might appear. Such kind secondary circulations might also induce the occurrence of urban local meteorological disasters, therefore the multi-scale feature and its effect of UHI is also a critical theoretical problem in the study of urban meteorological forecast methods. Computational analyses also reveal some correlation between the aerosol distribution in Beijing urban and outskirt areas and the multi-scale feature of UHI, i.e. the distributive feature of aerosols is similar to the multi-scale feature of UHI – Xicheng, Haidian, Shijingshan, Chaoyang Districts and the south of Chongwen District were the high value multi-centers area of PM_{10} concentrations (Figure omitted). The PM_{10} distributive feature also reveals that the secondary circulation and its convergent effect resulted from the multi-scale structure of UHI might induce the mesoscale aerosol transport, and local detention, concentration etc dynamical processes, thus forming the non-uniform distributive feature of aerosols.

6 Peripheral source influence of the UAP and the multi-scale spatial distributive feature of aerosols

According to the variation principle and its applied techniques, if the deviation field of MODIS AOD from the ground fixed and mobile measurements is $\Delta\tau(x,y)=\tau_M(x,y)-\tau_v(x,y)$, in terms of variation correction factor field function $\Delta\tilde{\tau}(x,y)$, functional J^* can be constructed to satisfy the following condition that J^* vanishes:

$$J^*=\iint\left\{(\Delta\tau-\Delta\tilde{\tau})^2+\lambda\left[\left(\frac{\partial\Delta\tau}{\partial x}\right)^2+\left(\frac{\partial\Delta\tau}{\partial y}\right)^2\right]\right\}dxdy\rightarrow\min, \tag{5}$$

where λ is a constraint coefficient. Expression (5) can be rewritten as

$$\delta J^*=\delta\sum\sum\left\{(\Delta\tau-D\tilde{\tau})^2+\lambda\left[\left(\frac{\partial\Delta\tau}{\partial x}\right)^2+\left(\frac{\partial\Delta\tau}{\partial y}\right)^2\right]\right\}=0, \tag{6}$$

Its corresponding Euler equation is

$$\Delta\tau-\Delta\tilde{\tau}-\tilde{\lambda}\left(\frac{\partial^2\Delta\tau}{\partial x^2}+\frac{\partial^2\Delta\tau}{\partial y^2}\right)=0, \tag{7}$$

where $\tilde{\lambda}$ is a constraint function. The above equations can be numerically solved using the iteration method to get the variation-corrected AOD field, $\tau_v(x,y)$.

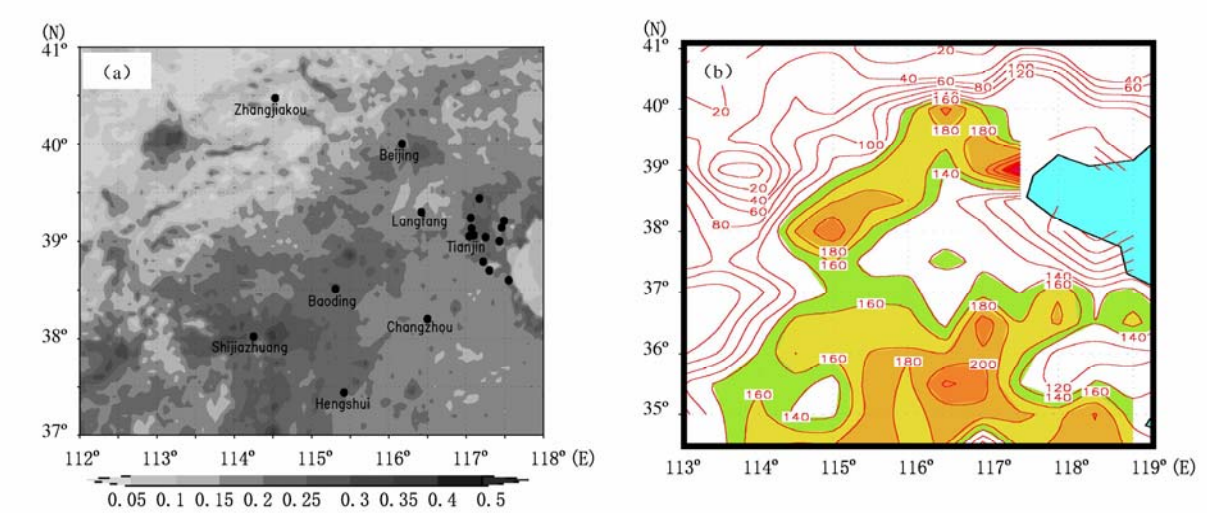

Fig.10 Composite surface PM_{10} variation-corrected MODIS AOD field under clear sky and stable weather condition (a) in the BECAPEX during January-February 2003, and the resident family number distribution (b; units: family·km^{-2}).

The variation-corrected field of surface photometer observation and Terra-MODIS AOD in winter 2002 preliminarily revealed the significant feature of the S-N zonal diffusion, transport, influence of aerosols between Beijing and its peripheral areas (Hebei, and Shandong provinces, etc)[30]. On this basis, the composite field (Fig.10(a)) of PM_{10} particle concentration variation-corrected MODIS AOD were calculated by using the BECAPEX MODIS AOD data under clear sky and stable weather condition in January-February 2003 and the surface PM_{10} particle concentration observations at Beijing, Hebei, and Tianjin, etc, it is found from the Figure that under the condition of clear sky and stable weather, the composite of the PM_{10}-corrected AOD also displayed a S-N "large triangle" shape aerosol influence

domain from Hebei, Shandong provinces, etc and Tianjin to Beijing urban area. The analysis of resident family number distribution (Fig.10(b)) exhibits an approximate S-N zonal pattern of the high family number area over Beijing, and its peripheral Tianjin, Hebei, Shandong etc provinces and cities, in accordance with the high value area of the AOD in Fig.10(a). Which might reflect the aerosol effect resulted from the emission and diffusion of the industrial and resident living's coal-burning pollution over the city agglomeration of Beijing, and its peripheral Tianjin, Hebei, Shandong etc.

On the basis of above S-N "large triangle" distributive feature of aerosols over Beijing and peripheral areas, in order to further understand the large-scale remote transport process of aerosols between Beijing and peripheral areas, and to trace the dispersion/transport track of peripheral source pollutants, the resultant correlation vector fields of the PM_{10} and $PM_{2.5}$ time series at Baishiqiao site and the NCEP/NCAR low level（925hPa）wind (u, v) field in February 2003 were calculated. The mathematical model of resultant correlation vector for tracing the dispersion track of pollutants is as the following:

$$\widetilde{R}(x,y) = \widetilde{R}_u(x,y)i + \widetilde{R}_v(x,y)j \ , \qquad (8)$$

where $\widetilde{R}$ is the resultant correlation vector of the observational site PM_{10} and $PM_{2.5}$ particle concentrations and the u and v component fields of wind, and $\widetilde{R}_u$ the CC field of the PM_{10} particle concentration series and u component, and $\widetilde{R}_v$ the CC field of the $PM_{2.5}$ particle concentration series and v component. It is found from Figs.11(a) and (b) that the emission sources of the PM_{10} and $PM_{2.5}$ particle matter observed at Baishiqiao site might be traced to Beijing's south peripheral area-Hebei, Shandong, and Tianjin etc, reflecting the large-scale transport feature of pollutants.

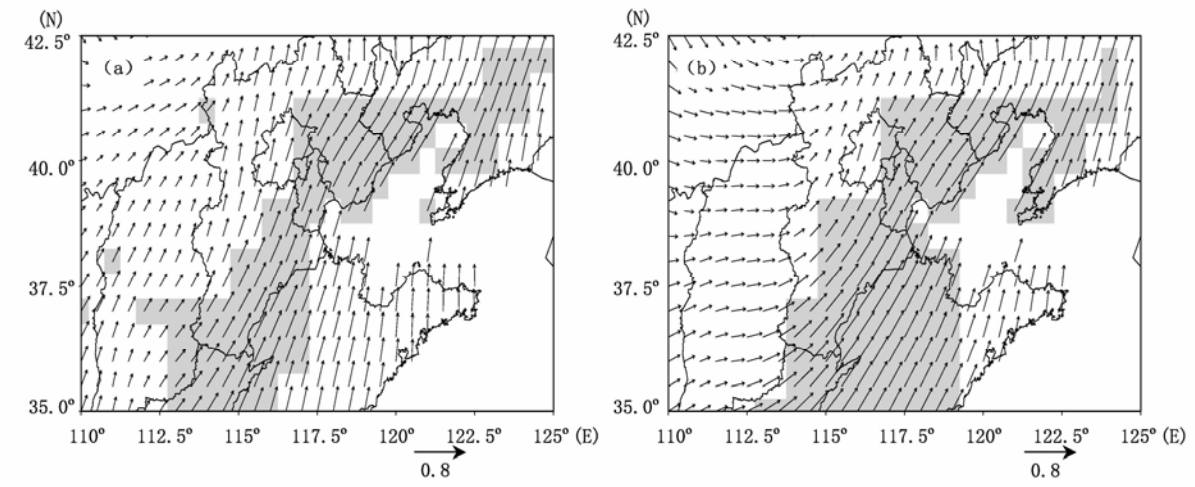

Fig.11 Resultant correlation vector fields of PM_{10} (a), $PM_{2.5}$ (b) concentrations observed at the Baishiqiao site and 925hPa wind field (u、v) in February 2003.;. Shaded areas denote where both $\tilde{R}_u$ and $\tilde{R}_v$ pass α =0.10 significant test.

The backward **t**rajectory analysis of air particles were carried out to trace the pollution transport/diffusion track of the peripheral emission sources of Beijing region by using the Hybrid Single-Particle Lagrangian Integrate Trajectory (HYSPLIT) model [31] developed by NOAA (ARL) Draxler et al. The version 4 (HYSPLIT-4) is an Eulerian—Lagrangian mixing computational model, its advection and diffusion are computed using the Lagrangian method, and the σ coordinate is used in the vertical direction:

$$\sigma = 1 - Z/Z_{top}, \qquad (9)$$

where Z is the height from the ground surface, Z_{top} the height of the top of the model. The horizontal grid of the model is the same with that of input meteorological element field; and the model is vertically divided into 28 layers, and meteorological elements are linearly interpolated onto each σ layer. The advection equations for trajectory computation are

$$P(t+\Delta t) = P(t) + 0.5[U(P,t) + U(P', t+\Delta t)]\Delta t , \quad (10)$$

$$P'(t+\Delta t) = P(t) + U(p,t)\Delta t , \quad (11)$$

where P is the position of air particle, P' the position variation of the particle caused by wind (horizontal and vertical) perturbations, U the wind speed, Δt the variable time step, and Δt<0.75 grid length/U_{max}（U_{max} is the maximum wind speed）.

The trajectory of air particle is calculated using the particle and puff mixing method [32], and horizontal and vertical diffusion equations are respectively:

$$X_{final}(t+\Delta t) = X_{mean}(t+\Delta t) + U'(t+\Delta t)\Delta t G , \quad (12)$$

$$Z_{final}(t+\Delta t) = Z_{mean}(t+\Delta t) + W'(t+\Delta t)\Delta t Z_{TOP}^{-1} , \quad (13)$$

their meaning is that the horizontal and vertical "mean" positions（X_{mean}, Z_{mean}）obtained under the action of mean flow plus the perturbation wind（U', W'）effect yield the final position of the particle at next time. The details of the model are referred to Draxler [33].

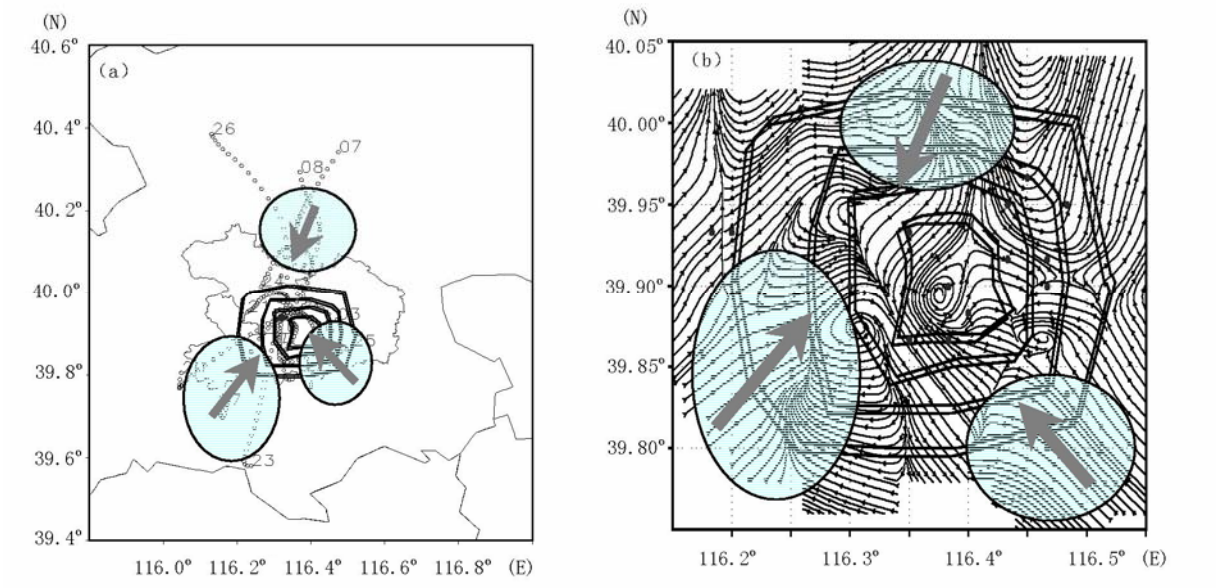

Fig.12 Simulation on the backward trajectory of air particle (a; 24 hrs, at 300 m height; numbers labeled on trajectories denote dates) on the February PM_{10} heavy pollution days (daily mean particle concentration≥180μg·m^{-3}) at Baishiqiao site in 2003 and the correlation vector field of PM_{10} concentration and filtered AWS wind field (b) in the peak value period (22:00-02:00 LT) of pollution.

The simulation on the backward trajectory of air particle (24 hrs, at 300 m height) on the winter PM_{10} heavy pollution days (daily mean particle concentration≥180μg·m^{-3}) at Baishiqiao site was performed in terms of the HYSPLIT-4 transport/diffusion model and using the mesoscale system analysis field separated

by a filter. It is found from the simulation that in eight out eleven samples, pollutants came from Beijing urban area or adjacent peripheral areas, i.e. through the southerly or southwest track of pollutant diffusion, and in three out of eleven samples, pollutants came through the northeasterly track from Beijing's suburban area (Fig.12(a)). This suggests that in Beijing urban heavy pollution events, the diffusion influence of close range suburban and peripheral sources might be mostly associated with suburban or southwest and south peripheral pollution sources.

According to the diurnal variation feature of winter PM_{10} concentration (Fig.2(a)), the hourly PM_{10} concentration in peak value period (22:00-02:00 LT) of pollution on urban PM_{10} heavy pollution days in February 2003 and the filtered 36 AWS stations wind field data were selected to calculate the correlation vector field depicting the transport/diffusion track of the particulate matter of atmospheric pollution on block-scale so as to explore the distribution of urban and peripheral sources and the diffusion effect of meso- and small-scale wind fields (Fig.12(b)), and it is found from the tracing and analysis results of the resultant correlation vector mathematical model (Expression 8) that the peak pollution concentration period on winter PM_{10} heavy pollution days at Baishiqiao site corresponded to the southwesterly correlation vector from the west suburb or "remote" transport and the southeasterly correlation vector, as well as the northerly correlation vector (arrows) from the northeast of the urban area. Which depicts the multi-scale transport feature of the far and close distances combination of atmospheric pollutants. The above result accords with the simulation of the backward trajectory of air particle using the HYSPLIT-4 transport/diffusion model and the filtering scheme on the whole (Figs.12 (a) and (b)).

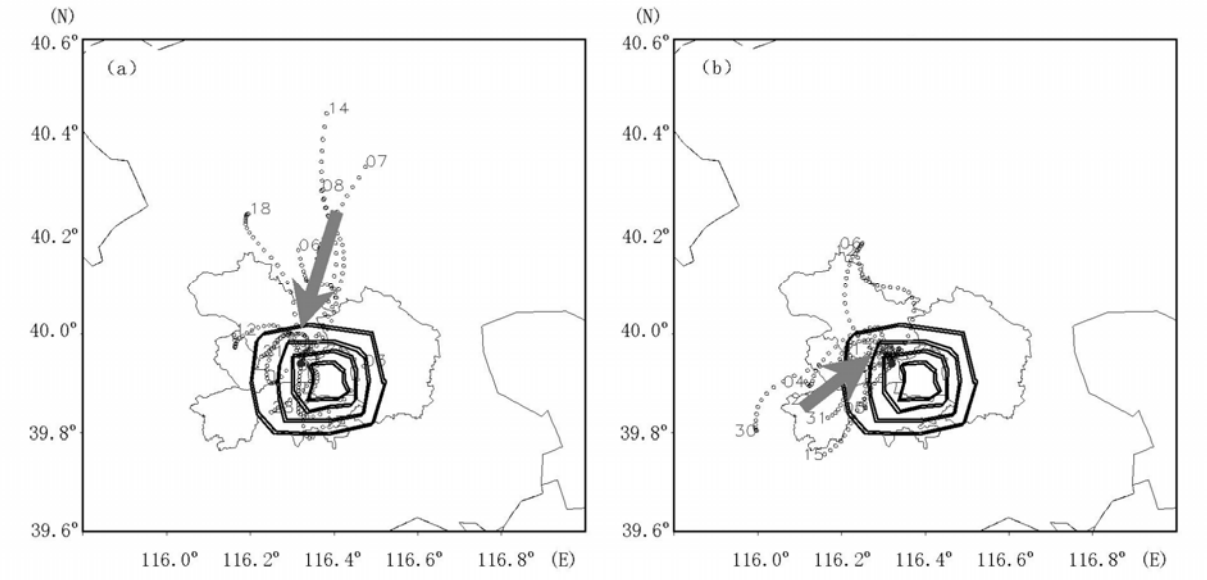

Fig.13 Simulation on the backward trajectory of air particle (24 hrs, at 300 m height) on the SO_2 heavy pollution days at Baishiqiao site in 2003. Numbers labeled on trajectories denote dates. (a) winter, February; (b) summer, August

Fig.13 displays the simulation of the backward trajectory of air particles on winter (February 2003)/summer (August 2003) SO_2 heavy pollution days (winter daily mean concentration $\geq 50\times10^{-9}$; summer $\geq 10\times10^{-9}$) at Baishiqiao Site by the HYSPLIT-4 transport/diffusion model and using the SO_2 heavy pollution day samples and filtered mesoscale wind field. It can be seen from Fig.13(a) that when urban SO_2 concentration was high, and under the filtered mesoscale weather system background, the simulated and analyzed backward trajectory of air particles came mainly from the northeast track from the outskirt, partly from the southeast track and the southwest track from the outskirt; while in summer, the backward trajectory came mainly from the southwest track from the outskirt, and partly from the southeast track or the northerly track (Fig.13(b)). Meanwhile, it can be also seen from Fig.13 that the spatial scale of the

diffusion effect of winter peripheral pollution sources was larger than one of summer, i.e. the transport distance of pollutants was larger in winter than in summer. The above computational results also reveal the seasonal differences of the city peripheral source's diffusion effect and pollution influence domain, and the multi-scale transport effect. The computational and analysis results of the correlation vector mathematical model for pollution source influence analysis, and the air particle trajectory simulation using the HYSPLIT-4 transport/diffusion model and its filtering scheme can be used to trace the peripheral pollution source distribution of UAP of different seasons and the multi-scale feature of their influence processes, and the above research and its methods provide scientific evidence and applied technical approach for the assessment of the overall effect of the regional atmospheric pollution sources of different "radii" of urban area and peripheral areas.

7 Regional features of atmospheric aerosol distribution in city and peripheral and its effect on cloud and fog

Studies [30, 34] indicated that under the background of prevail southerly wind, Beijing peripheral "U-shape" megarelief structure will retard the northward transport of pollutants from the south peripheral pollution sources, leading to the retardation of "migration" process of the atmospheric pollutants, and the short period "pile up" phenomenon. Obviously, under the comprehensive influence of the above geographic, climatic, and urban development situation etc aspects, the emission sources in peripheral areas (mainly Tianjin, Shijiazhuang, Baoding, Hengshui cities, etc in Hebei province, Shandong and Henan provinces, etc) might distinctively impact Beijing's atmospheric pollution status.

Fig.14 displays the winter mean TOMS AOD distribution over 1996-2002, it can be found from Fig.14 that the high value area of winter AOD showed a S-N zonal distribution over Beijing and its south peripheral area, and the aerosol high value area of Beijing region might extend to Hebei, Henan, Shandong, and Shanxi provinces, etc and a distinctive distribution feature along with topographic contours, indicating the close correlation between the pollution extent of the Beijing region within the valley megarelief and the pollution missions of peripheral various provinces. This makes us consider that will the persistent "pile up" of aerosols over the city agglomeration within such kind valley megarelief impact the regional climate of Beijing and peripheral areas?

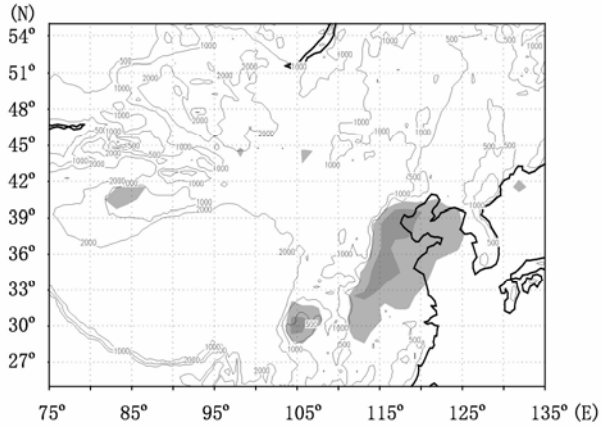

Fig.14 The distribution of winter mean TOMS AOD over 1996-2002, contours are topographic heights, and areas where AOD ≥0.4 are shaded.

Relevant studies [35-37] suggested that increase in aerosols might greatly impact sunshine and cloud and fog physical processes, thus leading to regional climate change. Therefore, meteorological stations within the high value area (114º~120ºE, 37º~41ºN) of TOMS AOD in Beijing and its peripheral in Fig.14 were

selected in this paper, whereon regional means of winter mean sunshine duration, low cloud cover (LCC), fog days, and AOD over 1979-2000 were calculated.

Fig.15 plots the temporal variations of regional mean winter sunshine duration and AOD, it can be seen from the Figure that winter AOD over Beijing and its periphery showed a distinctive increase trend (passing α=0.01 significant test) over 1979-2000, the sunshine duration a decline trend (passing α=0.10 significant test), and interannual "anti-phase" variation feature between the both is evident. This research result suggests that the regional decline feature of winter sunshine duration over Beijing-Tianjin and their south peripheral area in the recent 20-year to some extent reflected the local climate effect of aerosol radiative influence.

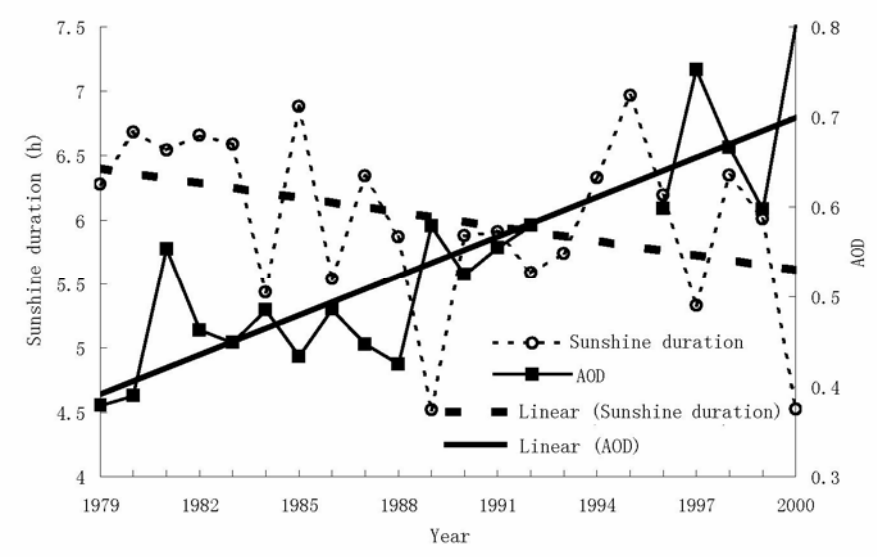

Fig.15 Comparison of winter mean sunshine duration and AOD variations over Beijing and peripheral areas in 1979~2000

The EOF decomposition is used to further analyze the principal spatial pattern (first eigenvector) and its ATC variation, and results show that in recent 20-year, the winter sunshine duration in north China turned from positive deviation to negative one, the LCC and fog day tended to increase, and the significant variation areas for various elements all lay in Beijing and its south peripheral area, showing a S-N zonal pattern, in accordance with the high value area of winter long-term mean AOD over Beijing and its peripheral areas. Those variation features prove that the regional climate change features of winter sunshine duration reduction and LCC and fog days increase in Beijing and its south peripheral area were close related with the direct and indirect radiative forcing of aerosols. It is found from analyzing the winter sunshine duration deviation field of the 1990s from the 1980s over Beijing and its peripheral cities that the sunshine duration of the 1990s over Beijing and peripheral areas all declined, and the low value center of the sunshine duration variation of Beijing and its south peripheral area in the deviation field corresponded well to the high value area of AOD, possibly reflecting the local climate effect of the radiative influence of aerosols. The winter LCC and fog day deviation fields of the 1990s from the 1980s show that winter mean urban fog days exhibited a significant increase trend in Beijing and its south peripheral area, and in particular, Beijing's southwest peripheral mountainous region was a high value deviation center of mean fog days; and the significant increase area of LCC lay in the south peripheral area of Bejing-Tianjin city agglomeration, appearing a S-N zonal pattern. Those interdecadal deviation features also reflect the indirect radiative forcing effect of aerosols close related with the pollution emission of winter industries and resident heating in the agglomeration. Besides, the south peripheral area lies in the downstream of winter dominant wind of Beijing-Tianjin agglomeration, the above distributive feature of the significant increase area of winter LCC and fog days might reflect the "plume" or " wake" effect of the downstream transport

of aerosols in atmospheric pollution processes of the agglomeration. For example, the hourly continuous measurement data of SO_2 and NO_2 concentrations and meteorological elements at the observation site of city meteorological administration in Haidian district in the BECAPEX in February 2001 were used to analyze the variations of pollutant concentration and condensation function in a persistent pollution process from smog to fog. It is found from comparing observed SO_2 concentrations with computed condensation function values that the low level SO_2 concentration had reached its maximum value before the occurrence of the heavy fog, its concentration was three times the early stage concentration; in the stage of fog occurrence and maintenance, the SO_2 concentration rapidly declined from the peak value, and the condensation function exhibited a distinctive increase trend. The sudden increase and decline laws of atmospheric SO_2 concentration before and after the occurrence of urban heavy fog showed an "anti-phase" variation feature with condensation function, that is to say, the condensation nuclei increase associated with the accumulation and sudden increase of SO_2 concentration in the low level played important role in the formation and development of urban fog. In this case of heavy fog, the analysis and computation results of NO_2 are similar to those of SO_2. The above research results reveal that the occurrence of exceptional persistent winter heavy fog over Beijing and north China was close related with the up-steam soot phenomenon observed in the early stage.

8 Multi-scale structure of UBL atmospheric pollution source influence

The spatial/temporal distribution of UAP is on one hand affected by urban and peripheral pollution source position (point source, surface source, and line source), and on the other hand by the multi-scale dynamical/thermal effects of urban building groups distribution, UHI, mountain and valley breeze or sea breeze, and urban climatic and diurnal variations, and seasonal feature [38]. Along with the development of city, the turbulence and thermal structure of underlying surface change, "canalization" appears between building groups on the two sides of urban peripheral ring-type roads (for example, Second Circle Road, Third Circle Road in Beijing), and the close- and distant- range pollutant transport from urban point and line (traffic pollution) sources and peripheral pollution emission source intensifies; besides, under the particular condition of urban atmospheric dynamical/thermal structure, the urban "air dome" resulted from the comprehensive effect of complex UBL might in turn complicate the UBL structure and pollutant distribution, thus forming a comprehensive physical image of the interaction of urban "air dome" dynamical structure and its dynamical-chemical process [39].

The comprehensive observation data of temperature, humidity, and O_3 concentration at different levels at Baishiqiao site in the BECAPEX in August 2003 were obtained using tethered sonde, and it is found that in the low level (below 300 m on average) of the UBL, the bottom of inversion layer, and the top of inverse humidity layer were significantly positively correlated with the height of the abrupt increase layer of O_3 concentration, indicating that atmospheric inversion/inverse humidity spatial structure was significantly correlated with the vertical distribution of O_3. The low level inversion/inverse humidity structure, and the vertical distribution feature of the high pollution area of urban low-level accompanied by the low O_3 layer depict that there existed some correlation among the vertical shear of wind, atmospheric thermal structure and aerosol pollution spatial distribution in the urban low level. The depth of the "near zero concentration" layer below the concentration-sharp-increase layer of O_3 may reflect the impact of summer NO_X etc gaseous pollutions on the consumption process of O_3, i.e. reflect the O_3-consumtion ability of urban low-level heavy pollution region. The depth might also depict the vertical spatial structure of the interaction, consumption, transformation, and vertical diffusion/mixing of various gaseous pollutants in the high concentration pollution region under the conditions of the inversion/inverse humidity within the urban building "canopy". The above results also describe the significant vertical spatial structure difference in the atmospheric pollutants concentration and their interaction in the UBL. The analysis of the meteorological

tower observations at the Institute of Atmospheric Physics, Chinese Academy of Science (IAP, CAS) in the BECAPEX shows that there was basically no association between PM_{10}/$PM_{2.5}$ concentrations and wind direction in the lowest 100 m of the UBL, but at 320 m there did exist the distinctive relation between southeast /southwest winds and the increase of aerosol concentration. Besides, according to the footprint analysis, in the low level below 100 m, the urban pollution source dominated, while at 320m height, the atmospheric pollution was very sensitive to the Hebei region emission source south of Beijing [40]. The above analysis conclusion describes that there existed different scale transport "influence layer" structure in the vertical in urban atmospheric pollution source impact processes, that is to say, the large-scale distant transport of peripheral source pollutants dominated the urban high level atmospheric pollution above 320 m, while urban-scale short-distance pollution source pollutants governed the urban low level pollution below 100m.

Computational results suggest that the low-level turbulent structure of Beijing UBL differed distinctively from one of other cities in China, i.e. the horizontal turbulent motion at the upper boundary of Beijing city agglomeration "canopy" showed a feature similar to fluctuant megarelief. Especially, the variances of the vertical speed fluctuation of UBL turbulence-scale motion in Beijing and Guangzhou were obviously larger than those in Nanjing, which is similar to the effect of fluctuant megarelief. This indicates that the fluctuation of vertical turbulence was strong in the low-level in Beijing city agglomeration, i.e. the dynamical effect of the vertical transport of turbulence was remarkable. Observations at the top (320m) of the tower show that the variances of the horizontal wind fluctuations in Beijing were far greater than those in other cities, plain topography, and similar to the overall effect of turbulences over fluctuant topography. This also reveals the "mountainous region effect" of turbulence-scale motion at the upper boundary of the Beijing city agglomeration "canopy"[41]. The above research conclusion depicts the significantly vertical difference in the spatial structure of turbulences in the urban surface layer. In the surface layer below 320 m, the vertical transport of sensible and latent heat was remarkable, and the thermal heterogeneity of the surface layer resulted in urban multiple flow convergent/divergent centers phenomenon, showing the multi-scale feature of flow field (secondary UHI effect). The vertical fluctuant component of the wind speed of low level urban turbulence motion was distinctive, and the horizontal fluctuant components in wind-resistance region were weak, therefore, the joint effect of the multi-scale effect of UHI group and the vertical transport dynamical effect of turbulences analogous to fluctuant topography effect within urban building ensemble "canopy" might lead to the non-uniform distribution of the local "pile up" and "retention" of urban atmospheric pollution. The area (320 m) aloft the city building ensemble was the large-scale distant transport region, i.e. the significant influence region of atmospheric pollution peripheral sources, while the low level of urban surface layer was the atmospheric pollution outskirt transport influence region. Due to the multi-scale effect of atmospheric dynamic structure and pollution process, urban aerosol concentration variations showed a multi-scale feature, with time scale ranging from several hours to several days, which was similar to the wind period spectrum of regional atmospheric dynamical structure.

The following multi-scale spatial structure model (Fig.16) for city agglomeration atmospheric pollution impact process can be summed up based on analyses results of the atmospheric pollution data obtained from atmospheric chemical observation systems at various sites in the BECAPEX, the observations of the vertical characters of surface layer turbulent structure at the IAP tower of 320 m, and the "point-surface" combined boundary layer comprehensive detecting system data.

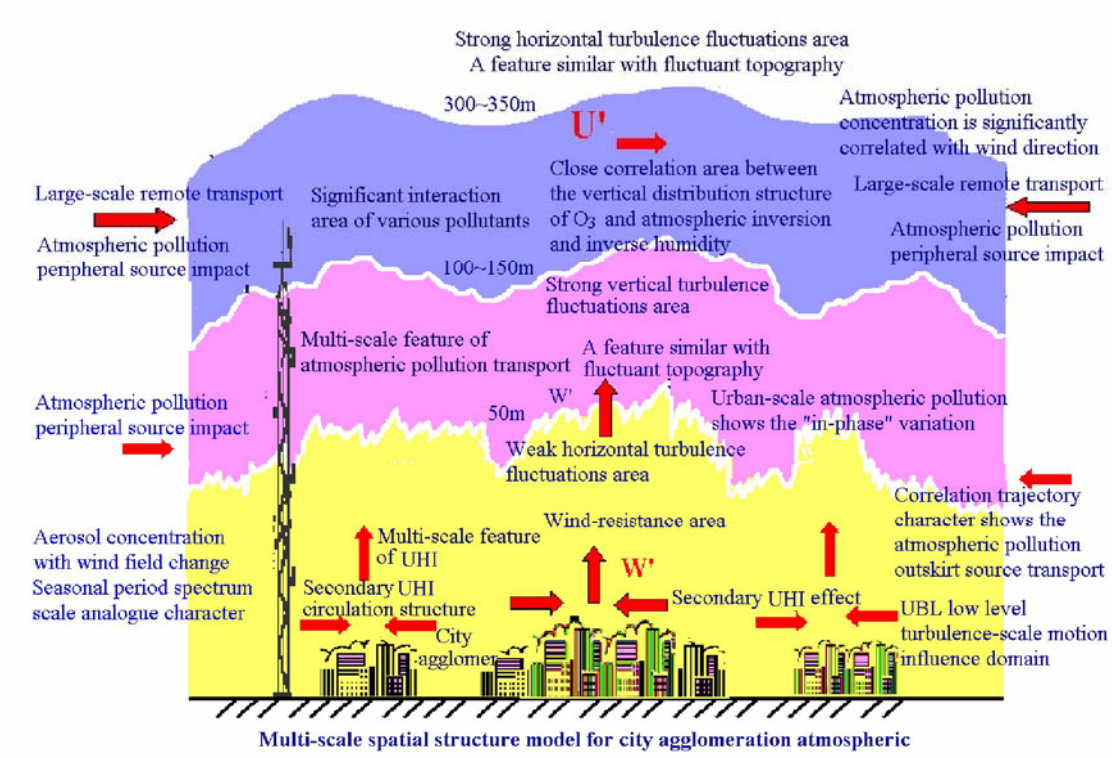

Fig.16 Multi-scale spatial structure model for city agglomeration atmospheric pollution impact process obtained from the comprehensive analysis of the BECAPEX data

9 Correlation feature of the spatial structure of atmospheric/soil pollution impact and water body environment

The effect of atmospheric/soil pollution on water quality in Miyun Reservoir is investigated in the BECAPEX through the comprehensive analysis of atmospheric dry/wet deposition character and hydrosphere, geosphere, and atmosphere. Research results indicate that the annual mean pH value of precipitation entering Miyun Reservoir in 1990~2003 appeared acidic, and exhibited an interannual decline trend. This indicates that the acidification extent of precipitation entering the reservoir gradually exacerbated. The mass concentration of falling dusts showed the distinctive seasonal variations, and the falling dust quantity in spring was the largest for spring sand storm weather. Elements in falling dusts and precipitation might exacerbate the eutrophication and potential heavy metal pollution of water body in the reservoir [42].

The statistical analysis results of the BECAPEX data suggest that there existed hydrosphere-geosphere-atmosphere pollution impact sources associated with summer local heavy precipitation in the Miyun Reservoir basin, and reveal the critical region for the water pollution within the Miyun Reservoir regional-scale range resulted from the upper-stream large-scale precipitation wash-out and confluent flow. The water quality change in the reservoir regional-scale range might be ascribed to the comprehensive effect of atmosphere-hydrosphere-geosphere mutual impact in the reservoir basin area spatial-scale range: the reservoir peripheral and distant ground surface floating dusts and blowing sands enter the atmosphere, directly fall into the reservoir through atmospheric dry/wet deposition, then impact reservoir water through various bio-chemical processes; the reservoir basin surface water, run-off, and ground water flow on ground surface or penetrates into the deep layer under the ground surface, after interact and exchange some substance with soil constituents, then converge into the reservoir, and this category water might change the pH value of reservoir water. The Miyun Reservoir basin is a complicated mountainous region, and the precipitation, and especially summer torrential rain wash-out of peripheral pollution sources severely

imperils the water quality of the reservoir. This kind mutual impact of multi-scale pollution sources can be described using the following concept model of hydrosphere, geosphere and atmospheric pollution impact sources (Fig.17).

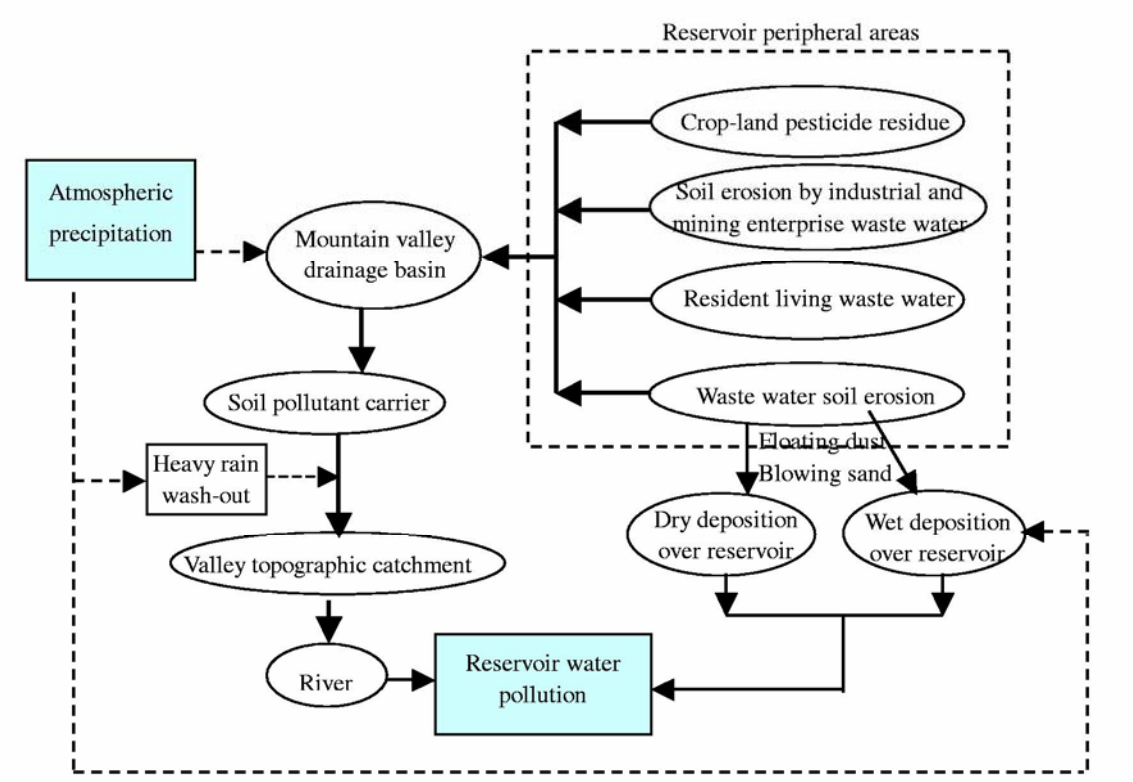

Fig.17 Concept model of atmosphere-geosphere-hydrosphere mutual impact in Reservoir

10 Conclusions

Based on the atmospheric pollution dynamic-chemical process structure observation data of the BECAPEX at observation sites in winter (February) and summer (August) 2003, and relevant meteorological elements, emission source, and satellite retrieval AOD etc comprehensive data, the spatial structure comprehensive analysis of atmospheric pollution source impact is performed in this paper in a "point-surface" combined way, so as to understand Beijing urban atmospheric pollution source influence domain and its scale feature, research analyses yield following concrete conclusions:

(1) The PCA of winter/summer particle concentration time series and various air pollutant concentration sample series suggests that the impacts of SO_2 and NO_X dominated the principal components of winter PM_{10} and $PM_{2.5}$ particle concentrations, while the impacts of CO and NO_X dominated in summer. The principal component "weight" coefficients of the winter/summer PM_{10} and $PM_{2.5}$ particle pollutant describe the seasonal difference of urban emission source impact.

(2) The "in-phase" variation feature of atmospheric pollution at the upper boundary of building ensemble in urban area might be correlated with the regional "in-phase" variation feature of urban surface layer dynamical and thermal factors. The synchronous variations of meteorological elements at different observation sites in urban area might provide a dynamic background condition for atmospheric pollution "in-phase" variation. The urban regional-scale atmospheric pollution "in-phase" variation law at different observation sites can be used to further develop new atmospheric pollution prediction method of "point-surface" combined technical approach, and provides the theoretical evidence for the application of atmospheric dynamic-chemical coupling model products and its statistical-dynamical technical method.

(3) PSA results reveal the periodic feature difference of winter/summer urban local wind field

variations, i.e. the large-scale system periodic feature in the winter local wind field is more significant than that in summer wind field. This seasonal periodic feature of atmospheric circulation system evolution might significantly affect the periodic feature of PM_{10} concentration variations, and lead to the particular long period variation process of winter atmospheric pollution differing from summer. The phenomenon also reveals that winter urban aerosol particle concentration variation processes have a longer decaying period than summer.

(4) Under the impact of the non-uniform feature of the multi-scale effect of urban building ensemble heat islands, the local convergent area of urban mesoscale low systems and the local UHI vertical circulation might form in the UBL. Such kind secondary circulations might also induce the occurrence of urban local meteorological disasters, therefore the multi-scale feature and its effect of UHI is also a critical theoretical problem in the study of urban meteorological forecast methods. Computational analyses also reveal some correlation between the aerosol distribution in Beijing urban and outskirt areas and the multi-scale feature of UHI, i.e. the distributive feature of aerosols is similar to the multi-scale feature of UHI. The secondary circulation and its convergent effect resulted from the multi-scale structure of UHI might induce the mesoscale aerosol transport, local detention, and conglomeration etc dynamical processes, thus forming the non-uniform distributive feature of aerosols.

(5) The high value distributive pattern of the surface PM_{10} concentration variation-corrected clear-sky MODIS satellite AOD composite corresponds to the high value area of the resident family number in Beijing and peripheral areas, reflecting the distant pollution source and large scale transport effects on Beijing winter urban aerosol particles. The computational and analysis results of the correlation vector mathematical model for pollution source influence analysis, and the air particle trajectory simulation using the HYSPLIT-4 transport/diffusion model and its filtering scheme can be used to trace the peripheral pollution source distribution of city atmospheric pollution of different seasons and the multi-scale feature of their influence processes, and the above research and its methods provide scientific evidence and applied technical approach for the assessment of the overall effect of the regional atmospheric pollution sources of different “radii” of urban area and peripheral areas.

(6) Base on comprehensive analyses, this paper presents the vertical structure of boundary turbulences in Beijing urban area, the spatial distributive feature of atmospheric pollution species interaction, and the multi-scale transport effect of atmospheric pollution source influence, as well as the multi-scale spatial structure model for city agglomeration atmospheric pollution source impact process.

(7) It is found from analyzing the winter mean TOMS AOD field that the high value area of winter AOD lay in Beijing and its south peripheral area, showing a distinctive feature of a S-N zonal distribution along the topographical contours. Winter AOD over Beijing and its periphery showed a distinctive increase trend over 1979-2000, the sunshine duration a decline trend, and interannual “anti-phase” variation feature between them is evident. While winter low cloud cover, fog days, AOD basically exhibited an interannual “in-phase” variation feature. This research result might reflect the local climate effect of aerosol influence.

(8) The atmospheric dry/wet deposition in the basin-scale distinctively affected the water body of Miyun Reservoir. A multi-scale mutual impact concept model for the influence of the multi-sphere pollution sources of hydrosphere, geosphere, and atmosphere associated with summer local heavy rain on the regional water quality of Miyun Reservoir is given based on the comprehensive analyses of the multi-sphere interaction of hydrosphere, geosphere, and atmosphere.

Acknowledgements This work was jointly supported by the Major State Basic Research Development Program 973 Project (Grant No. TG1999045700) and the International Sci-Tech Cooperative Project of Ministry of Science and Technology of the People´s Republic of China (Grant No. 2004DFA06100).

References

1. WMO, The Global Atmosphere Watch (GAW) Strategic Plan 2001-2007, 2001.
2. Apple, B. R., Berkeley visibility as related to atmospheric aerosol constituents, Atmos. Environ., 1985, 19 (9): 1525-1534.
3. James, F. S., Malm, W. C., The relative importance of soluble aerosols to spatial and seasonal trends of impaired visibility in the United States, Atmos Environ, 1994, 28 (5): 851-862.
4. Malm, W. C., Gebhart, K. A., Examining the relationship between atmospheric aerosols and light extinction at mount rainier and north cascades national parks, Atmos. Environ., 1994, 28 (2): 347-360.
5. Dupont, E., Carissimo, B., Pelon, J., et al, Comparison between the atmospheric boundary layer in Poris and its rural suburbs during the ECLAP experiment, Atmos. Environ., 1999, 33 (6): 979-994.
6. Ichinose, T., Hanaki, K., Shimodozono, K., Impact of atmospheric heat on urban climate in Tokyo, Atmos Environ, 1999, 33 (24): 3897-3909.
7. Romero, H., Rivera, A., Zalazar, P., et al, Rapid urban growth, land-use changes and air pollution in Santiago, Chile, Atmos. Environ., 1999, 33 (25): 4039-4047.
8. Okita, T., Estimation of direction of air flow from observation of rime jce, J. Meteor. Soc. Japan Ⅱ, 1960, 38 (4): 207-209.
9. Chandler, T. J., The climate of London, London: Hutchison, 1965. 1-71.
10. Lee, D. O., The influence of atmospheric stability and the urban heat island on urban-rural wind speed differences, Atmos. Environ., 1979, 13 (11): 1175-1180.
11. Oke, T. R., The energetic basis of the urban heat island, Quart. J. Roy Meteor. Soc., 1982, 108: 1-24.
12. Hanna, S. R., RAWSdell, J. V., Cramer, H. E., Urban Gaussian diffusion parameters. Modeling the urban boundary layer, Boston: Amer Meteor Soc, 1987, 337-379.
13. Qiao Zhiqi, Atmospheric Environment and Environmental Impact Assessment (in Chinese), Beijing: China Meteorological Press, 1998, 1-12.
14. Xu Xiangde, Influencing domain of peripheral sources in the urban heavy pollution process of Bijing, Science in China (ser. D), 2004, 34 (10): 958-966.
15. Zhang Zhigang, Gao Qingxian, Han Xueqin et al, The study of pollutants transport between the cities in north China, Research of Environmental Science (in Chinese), 2004, 17(1): 14-20.
16. Zhou Xiuji, Xu Xiangde, Yan Peng et al, Dynamic characteristics of spring sandstorms in 2000, Science in China (ser. D), 2002, 45 (10): 921-930.
17. Ren Zhenhai, Huang Meiyuan, Dong Baoqun et al, Study on Atmospheric Transport of Acidoid in China (in Chinese), Beijing：National Environment Protection Administration, 995, 1-27.
18. Zhao Deshan, Wang Minxin, Urban Pollution Atmospheric Aerosols of Coal Smoke type (in Chinese), Beijing: China Environmental Science Press, 1991, 55-58.
19. Hao Jiming, Wang Litao, Li Lin et al, Atmospheric pollution contribution rate associated with the energy source structure of Beijing city and regulating and controlling measure analysis, Science in China (ser. D), 2005, 35 (Supplement I):
20. Zhou Xiuji, Luo Chao, Ding Guoan et al., Preliminary analysis of the variations of surface ozone and nitric oxides in Lin'an, Acta Meteorologica Sinica, 1993, 7 (3): 287-294.
21. Yu Shuqiu, Lin Xuechun, Xu Xiangde, Spatial/temporal characteristics of atmospheric pollutants over the urban area of Beijing, Journal of Applied Meteorological Science (in Chinese), 2002, 13(Suppl.): 92-99.

22. An Junlin, Li Xin, Wang Yuesi et al, Measurements of atmospheric boundary layer O_3, NO_X and CO in summer with Beijing 325 m meteorological tower, Environmental Science (in Chinese), 2003, 24(6): 43-47.
23. Yan Fengqi, Hu Huanling, Wu Yonghua et al, Variation of aerosol parameters in summer and winter in Beijing, Research of Environmental Science (in Chinese), 2004, 17（1）：30-33.
24. Xu Xiangde, Ding Guoan, Zhou Li et al, Localized 3D-structural features of dynamic-chemical processes of urban air pollution in Beijing winter, Chinese Science Bulletin, 2003, 48(8): 819-825.
25. Ding Guoan, Meng Zhaoyang, Yu Haiqing et al, Measurement and Research on ABL air pollution in Beijing, Journal of Applied Meteorological Science (in Chinese), 2002, 13(Suppl.): 82-92.
26. Wang Minxin, Atmospheric Chemistry, Beijing: China Meteorological Press, 1999, 59-162.
27. Gao Zhiqiu, Bian Lingen, Lu Changgui et al, Estimation of aerodynamic parameters in urban areas, Journal of Applied Meteorological Science (in Chinese), 2002, 13 (Suppl.): 26-33.
28. Bian Lingen, Cheng Yanjie, Wang Xin et al, Observational study of wind and temperature profiles of urban boundary layer in Beijing winter, Journal of Applied Meteorological Science (in Chinese), 2002, 13 (Suppl.): 13-25.
29. Zhang Guangzhi, Xu Xiangde, Wang Jizhi et al, A study of characteristics and evolution of urban heat island over Beijing and its surrounding areas, Journal of Applied Meteorological Science (in Chinese), 2002, 13 (Suppl.): 43-50.
30. Xu Xiangde, Zhou Xiuji, Weng Yonghui et al, Study on variational aerosol fields over Beijing and its adjoining areas derived from Terra-MODIS and ground sunphotometer observation, Chinese Science Bulletin, 2003, 48(18): 2010-2017.
31. Draxler, R. R., Hess, G. D., An overview of HYSPLIT_4 modeling system for trajectories, dispersion and deposition, Aust. Meteor. Mag., 1998, 47: 295-308.
32. Hurley, P., PARTPUFF-A Lagrangian particle-puff approach for plume dispersion modeling applications, J. App. Meteor., 1994, 33: 285-294.
33. Draxler, R. R., Hess, G. D., Description of the HYSPLIT_4 modeling system, NOAA technical memorandum ERL ARL-224, 1997.
34. Xu Xiangde, Dynamic issues of urban atmospheric pollution models, Journal of Applied Meteorological Science (in Chinese), 2002, 13 (Suppl.): 1-12.
35. Kaiser, D. P., Qian, Y., Decrease trends in sunshine duration over China for 1954-1998: indication of increased haze pollution? Geophys. Res. Lett., 2002, 29(21):2042, doi:10.1029/2002GL016057.
36. Shen Qingji, Urban Ecology and Environment (in Chinese), Shanghai: Tongji University Press, 1998, 212-234.
37. Zhang Chengchang，Zhou Wenxian, An Introduction to Atmospheric Aerosols (in Chinese), Beijing: China Meteorological Press, 1995, 112-123.
38. Xu Xiangde, Tang Xu, An Introduction to Meteorology in Urbanization Environment (in Chinese). Beijing: China Meteorological Press, 2002, 1-10.
39. Xu Xiangde, Ding Guoan, Bian Lingen et al, Characteristics of atmospheric environment of boundary layer structure of city community in BECAPEX and integrate influence (in Chinese), Acta Meteorologica Sinica, 2004, 62 (5): 663-671.
40. Ding Guoan, Cheng Zunyu, Gao Zhiqiu et al, The vertical structure features of Beijing urban low level atmospheric PM_{10} and $PM_{2.5}$, Science in China (ser. D), 2005, 35 (Supplement I):
41. Zhou Mingyu, Yao Wenqing, Xu Xiangde, A study on vertical dynamical and thermal characteristics of urban boundary lower layer and its relationship with pollutant concentration in Beijing, Science in China (ser. D), 2005, 35 (Supplement I):
42. Yang Dongzhen, Xu Xiangde, Liu Xiaoduan et al, Complex Sources of Air-Soil-Water Pollution Processes in the Miyun Reservoir Region, Science in China (ser. D), 2005, 35(Supplement I):